Inorganic Chemistry
Article
Cite This: Inorg. Chem. XXXX, XXX, XXX−XXX
pubs.acs.org/IC

Syntheses and Structures of d^{10} Coinage Metal Complexes of Electron-Accepting Phosphine Ligands Featuring a 3,3,4,4,5,5-Hexafluorocyclopentene Framework

Tomohiro Agou,*[†] Nao Wada,[†] Kiyoshi Fujisawa,[‡] Takaaki Hosoya,[†] Yoshiyuki Mizuhata,[§] Norihiro Tokitoh,[§] Hiroki Fukumoto,*[†] and Toshio Kubota*[†]

[†]Department of Quantum Beam Science, Graduate School of Science and Engineering, Ibaraki University, 4-12-1, Nakanarusawa, Hitachi, Ibaraki 316-8511, Japan

[‡]Department of Chemistry, Faculty of Science, Ibaraki University, Mito, Ibaraki 310-8512, Japan

[§]Institute for Chemical Research, Kyoto University, Gokasho, Uji, Kyoto 611-0011, Japan

Supporting Information

ABSTRACT: Cu(I), Ag(I), and Au(I) complexes of monophosphine or bisphosphine ligands based on the 3,3,4,4,5,5-hexafluorocyclopentene skeleton were synthesized and structurally characterized by X-ray crystallographic analysis. The electron-withdrawing nature of these polyfluorinated phosphines was experimentally revealed via UV/vis absorption studies and crystal structure analysis. Successful catalytic application of the Au(I) complex for alkyne hydration reactions was investigated.

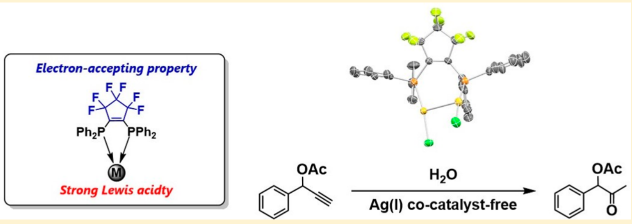

INTRODUCTION

d^{10} coinage-metal complexes have attracted considerable attention because of their unique structures, properties, and reactivities. These closed-shell metal complexes tend to form multinuclear structures consisting of M−X−M bridges (X is a halide, pseudohalide, or chalcogenide) and/or M- - -M metallophilic interactions.[1] Such d^{10} metal clusters often exhibit interesting properties such as long-wavelength absorptions and luminescence.[2]

Recently, catalytic usage of d^{10} coinage-metal complexes has been studied extensively. The strong Lewis acidity of the d^{10} coinage metals toward soft Lewis bases such as alkenes and alkynes enables unique molecular transformations.[3] In general, in order to enhance the Lewis acidity and catalytic activity of the d^{10} coinage-metal complexes, neutral precatalyst complexes must be transformed into catalytically active cationic complexes.[3a] An alternative approach to activation is the utilization of π-accepting ligands, which decrease the electron density of the metal ions and thus improve the Lewis acidity. For example, Ito et al. have reported that Au(I) complexes bearing strongly π accepting 3,4-diphosphinidenecyclobutene ligands catalyze the molecular transformations of alkynes without catalyst preactivation.[4]

Per- or polyfluorinated phosphines,[5] such as $P(C_6F_5)_3$[6] and $(C_6F_5)_2PCH_2CH_2P(C_6F_5)_2$,[7] are weakly σ donating and strongly π accepting ligands. These fluorinated phosphines have been utilized for catalytic reactions using late-transition-metal complexes,[8] despite limited structural variations. Furthermore, the steric hindrance of per- or polyfluorinated substituents such as C_6F_5 may destabilize the complexes and lower their catalytic performance. Therefore, phosphine ligands that have both π-accepting ability and less steric hindrance around the P atoms should be highly desirable in terms of the development of Lewis acid catalysts based on coinage-metal complexes.[9]

We previously reported the potential of hexafluorocyclopentene skeletons as scaffolds for polyfluorinated organic materials, including amorphous and low-refractive-index polymers,[10] electron-accepting molecules,[11] and π-conjugated polymers.[12] According to our research, the hexafluorocyclopentene skeleton is expected to be a key motif of the π-accepting and sterically compact phosphine ligands that are useful in the development of Lewis acidic transition-metal complexes. Previously, 1,2-bis(diphenylphosphino)hexafluorocyclopentene ("F_6PP")[13] and 1-(diphenylphosphino)-2-chlorohexafluorocyclopentene ("F_6P")[14] (Scheme 1) were used to synthesize transition-metal complexes (Fe,[13,15] Rh,[16] Cr,[17] Mo,[17] W,[17] Co[18]). Related hexafluorocyclopentene-bridged chiral bisphosphines were applied to Rh-catalyzed hydrogenation reactions of alkenes.[19] However, to the best of our knowledge, these polyfluorinated phosphine ligands have never been utilized to synthesize coinage-metal complexes. In addition, catalytic applications of these polyfluorinated phosphine-coordinated complexes have not been investigated fully.

In this paper, we describe the syntheses and structures of d^{10} coinage-metal complexes ofthe polyfluorinated bisphosphine

Received: April 23, 2018

DOI: 10.1021/acs.inorgchem.8b01111
Inorg. Chem. XXXX, XXX, XXX−XXX

Scheme 1. Syntheses of Coinage Metal Complexes 1−7 Bearing Polyfluorinated Phosphines F_6PP and F_6P

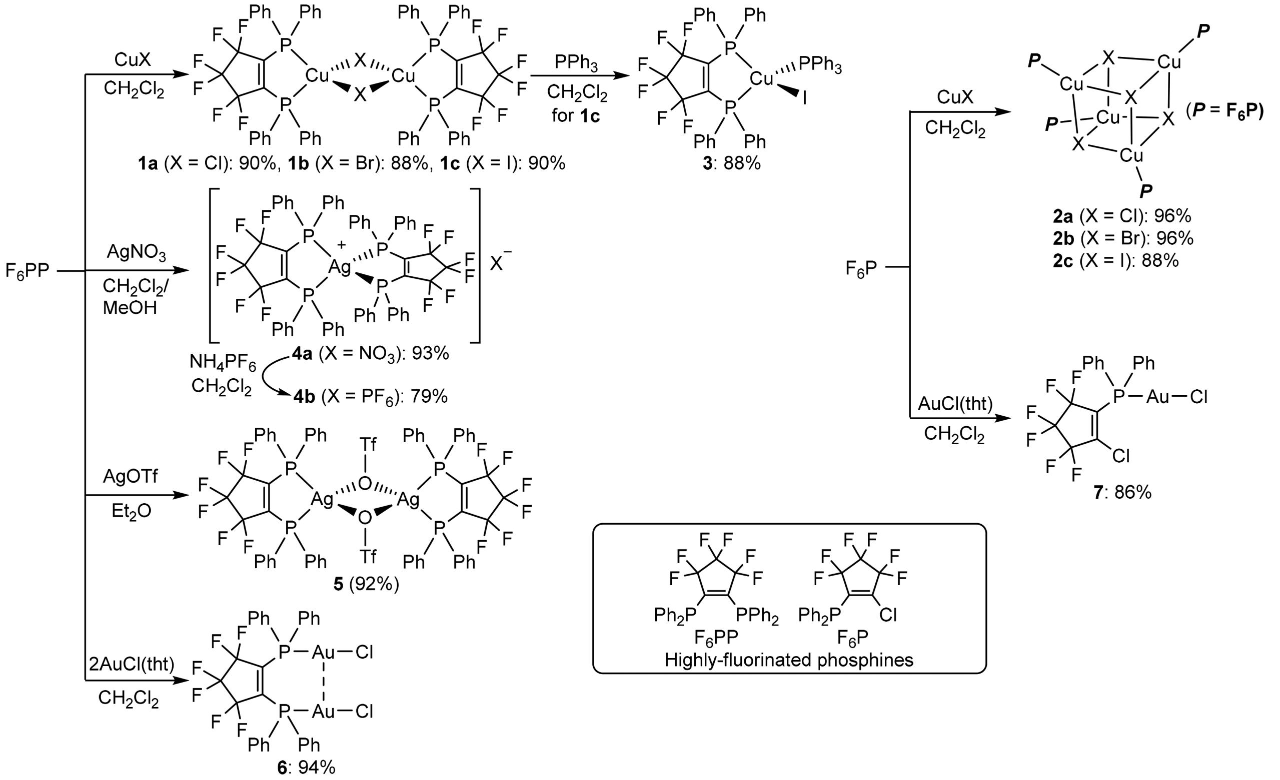

F_6PP and monophosphine F_6P (Scheme 1). The molecular structures were established by single-crystal X-ray crystallographic analyses, and the electronic structures were investigated via UV/vis absorption spectroscopy as well as density functional theory (DFT) calculations. The catalytic activity of the Au(I) complexes of F_6PP and F_6P was evaluated using an alkyne hydration reaction.[20]

■ EXPERIMENTAL SECTION

Materials and Instrumentation. All of the manipulations were performed under a dry argon atmosphere using Schlenk techniques. Materials obtained from commercial suppliers were used without further purifications. Et_2O and CH_2Cl_2 were purified by the Ultimate Solvent System from Glass Contour Co.[21] Preparative gel permeation chromatography (GPC) was carried out on a Shimadzu Prominence HPLC system equipped with Jaigel 1H+2H GPC columns using $CHCl_3$ as a solvent. ^1H, ^{13}C, ^{19}F, and ^{31}P NMR spectra were measured on a Bruker Avance-III 400 spectrometer, and chemical shifts are reported on the δ scale in ppm relative to tetramethylsilane (^1H and ^{13}C), $CFCl_3$ (^{19}F), or 85% H_3PO_4 (^{31}P). UV/vis spectra were recorded on a Shimadzu UV-3101PC spectrophotometer. Elemental analysis was carried out at the Instrumental Analysis Center, Ibaraki University, or at the Microanalytical Laboratory of the Institute for Chemical Research, Kyoto University. [AuCl(tht)] (tht = tetrahydrothiophene)[22] and 1-phenylprop-2-ynyl acetate (**8**)[23] were synthesized according to the literature procedures.

1,2-Bis(diphenylphosphino)-3,3,4,4,5,5-hexafluorocyclopentene (F_6PP).[13] To a Et_2O (10 mL) solution of 1,2-dichlorohexafluorocyclopentene (0.61 mL, 4.0 mmol) was added *n*-BuLi (1.6 M in hexane, 2.8 mL, 4.8 mmol) at −75 °C, and the mixture was stirred for 30 min. To the mixture was added $ClPPh_2$ (1.0 mL, 4.8 mmol). After the mixture was stirred for 1 h, it was treated with *s*-BuLi (1.0 M in cyclohexane, 4.8 mL, 4.8 mmol) and stirred for 30 min. After addition of $ClPPh_2$ (1.0 mL, 4.8 mmol), the mixture was stirred for 30 min and warmed to room temperature. After it was stirred for 1 h, the mixture was treated with saturated aqueous NH_4Cl, and the aqueous layer was extracted with CH_2Cl_2. The combined organic layer was dried over anhydrous $MgSO_4$, filtered, and concentrated under reduced pressure. The residue was recrystallized from CH_2Cl_2 to afford bisphosphine F_6PP as an orange solid (2.0 g, 3.6 mmol, 90%). ^1H NMR (400 MHz, $CDCl_3$, room temperature): δ 7.22−7.32 (m, 20H). $^{13}C\{^1H\}$ NMR (100 MHz, $CDCl_3$, room temperature): δ 134.3 (t, J = 11.8 Hz), 129.6 (s), 128.5 (t, J = 3.9 Hz). ^{13}C NMR signals attributable to the hexafluorocyclopentene moiety and the *ipso* carbon atoms of the Ph groups could not be observed. ^{19}F NMR (376 MHz, $CDCl_3$, room temperature): δ −105.6 (s, 4F), −132.6 (quint, J = 6.9 Hz, 2F). $^{31}P\{^1H\}$ NMR (128 MHz, $CDCl_3$, room temperature): δ −21.3 (s).

1-Diphenylphosphino-2-chloro-3,3,4,4,5,5-hexafluorocyclopentene (F_6P).[14] To a Et_2O (10 mL) solution of 1,2-dichlorohexafluorocyclopentene (0.61 mL, 4.0 mmol) was added *n*-BuLi (1.6 M in hexane, 2.8 mL, 4.8 mmol) at −75 °C, and the mixture was stirred for 30 min. To the mixture was added $ClPPh_2$ (1.0 mL, 4.8 mmol). After the mixture was stirred for 1 h, it was warmed to room temperature. After it was stirred for 3 h, the mixture was treated with saturated aqueous NH_4Cl, and the aqueous layer was extracted with CH_2Cl_2. The combined organic layer was dried over anhydrous $MgSO_4$, filtered, and concentrated under reduced pressure. The residue was separated by using GPC to afford phosphine F_6P as a yellow solid (1.4 g, 3.4 mmol, 85%). ^1H NMR (400 MHz, $CDCl_3$, room temperature): δ 7.38−7.44 (m, 10H). $^{13}C\{^1H\}$ NMR (100 MHz, $CDCl_3$, room temperature): δ 134.4 (s), 134.2 (s), 130.3 (s), 128.9 (d, J = 8.6 Hz). ^{13}C NMR signals attributable to the hexafluorocyclopentene moiety could not be observed. ^{19}F NMR (376 MHz, $CDCl_3$, room temperature): δ −104.5 (m, 2F), −114.1 (m, 2F), −130.2 (m, 2F). $^{31}P\{^1H\}$ NMR (128 MHz, $CDCl_3$, room temperature): δ −20.2 (s).

$[CuCl(F_6PP)]_2$ (1a). To a slurry of CuCl (0.10 g, 1.0 mmol) in CH_2Cl_2 (65 mL) was added F_6PP (0.54 g, 1.0 mmol), and the resulting solution was stirred for 1 day. The solution was filtered and evaporated. The residue was recrystallized from CH_2Cl_2 to afford **1a** as orange crystals (0.58 g, 0.45 mmol, 90%). ^1H NMR (400 MHz, $CDCl_3$, room temperature): δ 7.46−7.41 (dd, J = 6.6, 6.2 Hz, 16H); 7.27 (t, J = 7.5 Hz, 8H), 7.13 (t, J = 7.8 Hz, 16H). ^{19}F NMR (376

MHz, $CDCl_3$, room temperature): δ −106.6 (s, 8F), −132.4 (s, 4F). $^{31}P\{^1H\}$ NMR (128 MHz, $CDCl_3$, room temperature): δ −21.6 (br s). UV/vis (CH_2Cl_2, room temperature): λ_{max} 468 nm ($\varepsilon = 1.8 \times 10^3$ M^{-1} cm^{-1}). Anal. Calcd for $C_{58}H_{40}Cl_2Cu_2F_{12}P_4$: C, 54.14; H, 3.13. Found: C, 54.03; H, 3.34.

$[CuBr(F_6PP)]_2$ (1b). To a slurry of CuBr (0.14 g, 1.0 mmol) in CH_2Cl_2 (50 mL) was added F_6PP (0.55 g, 1.0 mmol), and the resulting solution was stirred for 1 day. The solution was filtered and evaporated. The residue was recrystallized from CH_2Cl_2 to afford **1b** as orange crystals (0.69 g, 0.44 mmol, 88%). ^1H NMR (400 MHz, $CDCl_3$, room temperature): δ 7.40 (dd, *J* = 6.5, 6.3 Hz, 16H), 7.27 (t, *J* = 7.5 Hz, 8H), 7.13 (t, *J* = 7.5 Hz, 16H). ^{19}F NMR (376 MHz, $CDCl_3$, room temperature): δ −106.5 (s, 8H), −132.2 (s, 4F). $^{31}P\{^1H\}$ NMR (128 MHz, $CDCl_3$, room temperature): δ −23.7 (br s). UV/vis (CH_2Cl_2, room temperature): λ_{max} 462 nm ($\varepsilon = 1.9 \times 10^3$ M^{-1} cm^{-1}). Anal. Calcd for $C_{58}H_{40}Br_2Cu_2F_{12}P_4$: C, 50.64; H, 2.93. Found: C, 50.71; H, 3.18.

$[CuI(F_6PP)]_2$ (1c). To a slurry of CuI (0.19 mg, 1.0 mmol) in CH_2Cl_2 (65 mL) was added F_6PP (0.55 g, 1.0 mmol), and the resulting solution was stirred for 1 day in the absence of light. The solution was filtered and evaporated. The residue was recrystallized from CH_2Cl_2 to afford **1c** as yellow crystals (0.66 g, 045 mmol, 90%). ^1H NMR (400 MHz, $CDCl_3$, room temperature): δ 7.38 (dd, *J* = 6.0, 5.8 Hz, 16H), 7.27 (t, *J* = 7.6 Hz, 8H); 7.12 (t, *J* = 7.6 Hz, 16H). ^{19}F NMR (376 MHz, $CDCl_3$, room temperature): δ −106.5 (s, 8F), −132.2 (s, 4F). $^{31}P\{^1H\}$ NMR (128 MHz, $CDCl_3$, room temperature): δ −27.1 (br s). UV/vis (CH_2Cl_2, room temperature): λ_{max} 454 nm ($\varepsilon = 1.3 \times 10^3$ M^{-1} cm^{-1}). Anal. Calcd for $C_{58}H_{40}Cu_2F_{12}I_2P_4$: C, 47.40; H, 2.74. Found: C, 47.76; H, 2.91.

$[CuCl(F_6P)]_4$ (2a). To a slurry of CuCl (0.10 g, 1.0 mmol) in CH_2Cl_2 (65 mL) was added F_6P (0.20 g, 0.50 mmol), and the resulting solution was stirred for 1 day. The solution was filtered and evaporated. The residue was recrystallized from CH_2Cl_2 to afford **2a** as yellow crystals (0.23 g, 0.12 mmol, 96%). ^1H NMR (400 MHz, $CDCl_3$, room temperature): δ 7.76 (dd, *J* = 7.8, 4.6 Hz, 16H), 7.45 (t, *J* = 7.3 Hz, 8H), 7.36 (t, *J* = 7.6 Hz, 16H). ^{19}F NMR (376 MHz, $CDCl_3$, room temperature): δ −104.2 (s, 8F), −114.0 (s, 8F), −130.0 (s, 8F). $^{31}P\{^1H\}$ NMR (128 MHz, $CDCl_3$, room temperature): δ −17.3 (br s). UV/vis (CH_2Cl_2, room temperature): λ_{max} 344 nm ($\varepsilon = 6.5 \times 10^3$ M^{-1} cm^{-1}). Anal. Calcd for $C_{68}H_{40}Cl_8Cu_4F_{24}P_4$: C, 41.36; H, 2.04. Found: C, 41.52; H, 2.34.

$[CuBr(F_6P)]_4$ (2b). To a slurry of CuBr (0.14 g, 1.0 mmol) in CH_2Cl_2 (65 mL) was added F_6P (0.20 g, 0.50 mmol), and the resulting solution was stirred for 1 day. The solution was filtered and evaporated. The residue was recrystallized from CH_2Cl_2 to afford **2b** as yellow crystals (0.26 g, 0.12 mmol, 96%). ^1H NMR (400 MHz, $CDCl_3$, room temperature): δ 7.76 (dd, *J* = 7.8, 4,6 Hz, 16H), 7.47 (t, *J* = 7.3 Hz, 8H), 7.36 (t, *J* = 7.6 Hz, 16H). ^{19}F NMR (376 MHz, $CDCl_3$, room temperature): δ −104.2 (s, 8F), −113.7 (s, 8F), −129.7 (s, 8F). $^{31}P\{^1H\}$ NMR (128 MHz, $CDCl_3$, room temperature): δ −20.3 (br s). UV/vis (CH_2Cl_2, room temperature): λ_{max} 350 nm ($\varepsilon = 6.4 \times 10^3$ M^{-1} cm^{-1}). Anal. Calcd for $C_{68}H_{40}Br_4Cl_4Cu_4F_{24}P_4$: C, 37.94; H, 1.87. Found: C, 38.93; H, 2.16.

$[CuI(F_6P)]_4$ (2c). To a slurry of CuI (0.19 g, 1.0 mmol) in CH_2Cl_2 (65 mL) was added F_6P (0.20 g, 0.50 mmol), and the resulting solution was stirred for 1 day in the absence of light. The solution was filtered and evaporated. The residue was recrystallized from CH_2Cl_2 to afford **2c** as yellow crystals (0.27 g, 0.11 mmol, 88%). ^1H NMR (400 MHz, $CDCl_3$, room temperature): δ 7.76 (dd, *J* = 7.9, 5.6 Hz, 16H), 7.66 (t, *J* = 7.4 Hz, 8H), 7.54−7.58 (m, 16H). ^{19}F NMR (376 MHz, $CDCl_3$, room temperature): δ −104.1 (s, 8F), −113.5 (s, 8F), −129.5 (s, 8F). $^{31}P\{^1H\}$ NMR (128 MHz, $CDCl_3$, room temperature): δ −29.8 (br s). UV/vis (CH_2Cl_2, room temperature): λ_{max} 364 nm ($\varepsilon = 9.6 \times 10^3$ M^{-1} cm^{-1}). Anal. Calcd for $C_{68}H_{40}I_4Cl_4Cu_4F_{24}P_4$: C, 34.90; H, 1.72. Found: C, 35.93; H, 1.82.

$[CuI(F_6PP)(PPh_3)]$ (3). To a solution of $[CuI(F_6PP)]_2$ (**1c**; 38 mg, 0.026 mmol) in CH_2Cl_2 (5 mL) was added PPh_3 (14 mg, 0.052 mmol), and the resulting solution was stirred for 1 day. The solution was filtered and evaporated. The residue was recrystallized from CH_2Cl_2 to afford **3** as yellow crystals (46 mg, 0.046 mmol, 88%). ^1H NMR (400 MHz, $CDCl_3$, room temperature): δ 6.88−7.96 (m, 35H). ^{19}F NMR (376 MHz, $CDCl_3$, room temperature): δ −104.4 (d, *J* = 270.0 Hz, 2F), −109.1 (d, *J* = 270.0 Hz, 2F), −130.1 (d, *J* = 232.0 Hz, 1F), −132.9 (d, *J* = 232.0 Hz, 1F). $^{31}P\{^1H\}$ NMR (128 MHz, $CDCl_3$, room temperature): not observed. UV/vis (CH_2Cl_2, room temperature): λ_{max} 426 nm ($\varepsilon = 6.6 \times 10^2$ M^{-1} cm^{-1}). Anal. Calcd for $C_{47}H_{35}CuF_6IP_3\cdot CH_2Cl_2$: C, 53.28; H, 3.45. Found: C, 53.18; H, 3.47. Presence of CH_2Cl_2 molecules in the crystals was confirmed by X-ray crystallographic analysis.

$[Ag(F_6PP)_2](NO_3)$ (4a). To a solution of $AgNO_3$ (34 mg, 0.20 mmol) in MeOH (10 mL) was added a solution of F_6PP (0.11 g, 0.20 mmol) in CH_2Cl_2 (10 mL), and the resulting solution was stirred for 1 day in the absence of light. The solution was filtered and evaporated. The residue was recrystallized from CH_2Cl_2 to afford **4a** as yellow crystals (0.12 g, 0.093 mmol, 93%). ^1H NMR (400 MHz, $CDCl_3$, room temperature): δ 7.12−7.32 (m, 40H). ^{19}F NMR (376 MHz, $CDCl_3$, room temperature): δ −105.3 (s, 8F), −132.5 (s, 4F). $^{31}P\{^1H\}$ NMR (128 MHz, $CDCl_3$, room temperature): δ −17.9 (br s). UV/vis (CH_2Cl_2, room temperature): λ_{max} 378 nm ($\varepsilon = 2.0 \times 10^3$ M^{-1} cm^{-1}). Anal. Calcd for $C_{58}H_{40}AgF_{12}NO_3P_4$: C, 55.35; H, 3.20. Found: C, 55.22; H, 3.35.

$[Ag(F_6PP)_2](PF_6)$ (4b). To a solution of $[Ag(F_6PP)_2](NO_3)$ (**4a**; 30 mg, 0.024 mmol) in CH_2Cl_2 (5 mL) was added NH_4PF_6 (3.9 mg, 0.024 mmol), and the resulting solution was stirred for 1 day in the absence of light and extracted with CH_2Cl_2. The organic layer was dried over anhydrous $MgSO_4$, filtered, and concentrated under reduced pressure. The residue was recrystallized from $CHCl_3$ to afford **4b** as yellow crystals (26 mg, 0.019 mmol, 79%). ^1H NMR (400 MHz, $CDCl_3$, room temperature): δ 7.19−7.26 (m, 40H). ^{19}F NMR (376 MHz, $CDCl_3$, room temperature): δ −73.6 (d, *J* = 714.0 Hz, 6F, PF_6), −105.7 (s, 8F), −133.1 (s, 4F). $^{31}P\{^1H\}$ NMR (128 MHz, $CDCl_3$, room temperature): not observed. UV/vis (CH_2Cl_2, room temperature): λ_{max} 376 nm ($\varepsilon = 2.1 \times 10^3$ M^{-1} cm^{-1}). Anal. Calcd for $C_{58}H_{40}AgF_{18}P_5$: C, 51.92; H, 3.01. Found: C, 52.14; H, 3.25.

$[Ag(F_6PP)(OTf)]_2$ (5). To a solution of F_6PP (54 mg, 0.10 mmol) in Et_2O (5 mL) was added AgOTf (26 mg, 0.10 mmol), and the resulting solution was stirred for 1 day in the absence of light. The solution was filtered and evaporated. The residue was recrystallized from CH_2Cl_2 to afford **5** as yellow crystals (74 mg, 0.046 mmol, 92%). ^1H NMR (400 MHz, $CDCl_3$, room temperature): δ 7.34−7.43 (m, 24H), 7.30 (t, *J* = 7.2 Hz, 16H). ^{19}F NMR (376 MHz, $CDCl_3$, room temperature): δ −77.0 (s, 6F, CF_3SO_3), −105.1 (s, 8F), −132.5 (s, 4F). $^{31}P\{^1H\}$ NMR (128 MHz, $CDCl_3$, room temperature): δ −13.8 (s). UV/vis (CH_2Cl_2, room temperature): λ_{max} 376 nm ($\varepsilon = 2.5 \times 10^2$ M^{-1} cm^{-1}). Anal. Calcd for $C_{60}H_{40}Ag_2F_{18}O_6P_4S_2$: C, 44.97; H, 2.52. Found: C, 44.86; H, 2.75.

$[Au_2Cl_2(F_6PP)]$ (6). To a solution of [AuCl(tht)] (64 mg, 0.20 mmol) in CH_2Cl_2 (5 mL) was added F_6PP (54 mg, 0.10 mmol), and the resulting solution was stirred for 1 day. The solution was filtered and evaporated. The residue was recrystallized from CH_2Cl_2 to afford **6** as yellow crystals (95 mg, 0.094 mmol, 94%). ^1H NMR (400 MHz, $CDCl_3$, room temperature): δ 7.56−7.61 (m, 12H), 7.47 (t, *J* = 7.5 Hz, 8H). ^{19}F NMR (376 MHz, $CDCl_3$, room temperature): δ −104.6 (t, *J* = 5.6 Hz, 4F), −132.8 (t, *J* = 5.6 Hz, 2F); $^{31}P\{^1H\}$ NMR (128 MHz, $CDCl_3$, room temperature): δ 16.0 (s). UV/vis (CH_2Cl_2, room temperature): λ_{max} 368 nm ($\varepsilon = 7.4 \times 10^2$ M^{-1} cm^{-1}). Anal. Calcd for $C_{29}H_{20}Au_2Cl_2F_6P_2$: C, 34.51; H, 2.00. Found: C, 33.99; H, 2.17.

$[AuCl(F_6P)]$ (7). To a solution of [AuCl(tht)] (45 mg, 0.14 mmol) in CH_2Cl_2 (5 mL) was added F_6P (55 mg, 0.14 mmol), and the resulting solution was stirred for 1 day. The solution was filtered and evaporated. The residue was recrystallized from CH_2Cl_2 to afford **7** as colorless crystals (76 mg, 0.12 mmol, 86%). ^1H NMR (400 MHz, $CDCl_3$, room temperature): δ 7.63−7.72 (m, 6H), 7.54−7.59 (m, 4H). ^{19}F NMR (376 MHz, $CDCl_3$, room temperature): δ −103.6 (s, 2F), −114.2 (s, 2F), −130.0 (s, 2F). $^{31}P\{^1H\}$ NMR (128 MHz, $CDCl_3$, room temperature): δ 16.1 (s). Anal. Calcd for $C_{17}H_{10}AuCl_2F_6P$: C, 32.56; H, 1.61. Found: C, 32.74; H, 1.68.

Catalytic Hydration of Acetate 8. To a solution of **6** (30 mg, 0.030 mmol) was added a solution of acetate **8** (0.17 g, 1.0 mmol) in 1,4-dioxane (7.5 mL) and H_2O (2.5 mL). After it was stirred at 25 °C for 24 h, the mixture was subjected to column chromatography (hexane/EtOAc, 4/1) to afford 2-oxo-1-phenylpropyl acetate (**9**) as a colorless oil (98 mg, 0.51 mmol, 51%). ^{1}H NMR (400 MHz, $CDCl_3$, room temperature): δ 7.41 (s, 5H), 5.97 (s, 1H), 2.20 (s, 3H), 2.11 (s, 3H). The spectral data of **9** were identical with those reported previously.[20]

X-ray Crystallographic Analysis. Single crystals were immersed in cryo-oil, mounted on a MicroMount, and measured at a temperature of 173 K. X-ray diffraction data were recorded on a Rigaku XtaLabMini diffractometer using graphite-monochromated Mo Kα radiation (λ = 0.71075 Å) at 173 K or on a Rigaku Saturn 724 CCD diffractometer equipped with the VariMax optic system using Mo Kα radiation (λ = 0.71075 Å) at 173 K. The reflection data were integrated, scaled, and averaged by using CrysAlisPro (ver. 1.171.38.46). Empirical absorption corrections were applied using the SCALE3 ABSPACK scaling algorithm (CrysAlisPro). The structures were solved by direct methods (SHELXT-2014/5) and refined by full-matrix least-squares methods on F^2 for all reflections (SHELXL-2016/6).[24] All hydrogen atoms were placed using AFIX instructions, while all of the other atoms were refined anisotropically. In the X-ray diffraction measurements and the crystallographic analysis of **1a**, **2b**,**c**, **4a**,**b**, and **7**, we encountered problems owing to the poor crystal quality and/or twinning, and special treatments were necessary. The details are described in the Supporting Information.

Crystallographic data for the newly synthesized compounds have been deposited with the Cambridge Crystallographic Data Centre. These data can be obtained free of charge from the Cambridge Crystallographic Data Centre via www.ccdc.cam.ac.uk/data_request/cif.

Computational Details. All calculations were performed using the Gaussian 16 (rev. A.03) program package.[25] Geometry optimizations were performed at the B3PW91/6-31G(d) (Au, Ag, Cu, I: SDD) level of theory including the D3 version of Grimme's empirical dispersion (B3PW91-D3).[26] The frequency calculations confirmed that all of the optimized geometries corresponded to the equilibrium structures. Excited energies and oscillator strengths were calculated on the optimized structures by the TD-DFT method at the B3PW91/6-31+G(d) (Au, Ag, Cu, I: SDD) level. Molecular structures and Cartesian coordinates of the optimized structures are included in the Supporting Information.

RESULTS AND DISCUSSION

Synthesis and Structural Characterization. *Fluorinated Phosphines.* To begin, the syntheses of polyfluorinated bisphosphine F_6PP and monophosphine F_6P were reinvestigated because the literature methods are not ideal due to extended reaction times and low yields.[13,14] By taking advantage of the Li−Cl exchange reaction of 1,2-dichloro-3,3,4,4,5,5-hexafluorocyclopentene,[27] we readily obtained F_6PP in high yield (Scheme 2). Monophosphine F_6P was also obtained via the same method. It is worth noting that phosphines F_6PP and F_6P are not easily oxidized, even by treatment with excess aqueous H_2O_2, suggesting a weak σ-donating ability of the P atoms in these phosphines.

Scheme 2. Preparation of Phosphines F_6PP and F_6P

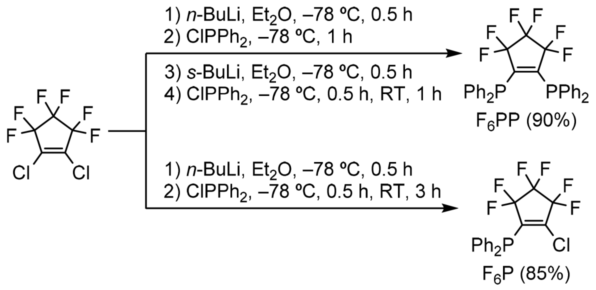

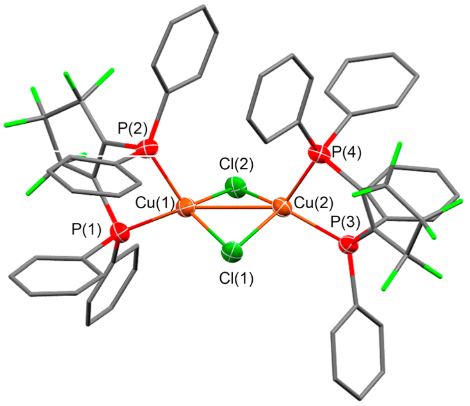

Figure 1. Structure of **1a**·CH_2Cl_2. Thermal ellipsoids are drawn at the 50% probability level. Hydrogen atoms, disordered fluorine atoms, and solvent molecule are omitted for clarity.

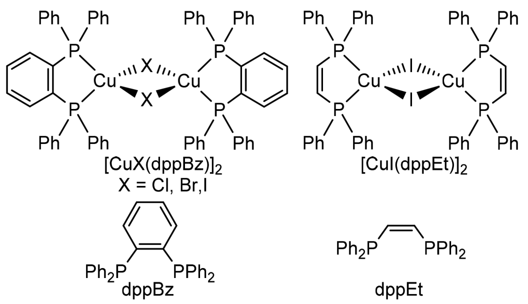

Figure 2. Representative dinuclear Cu(I) complexes bearing chelating bisphosphines (refs 29 and 30).

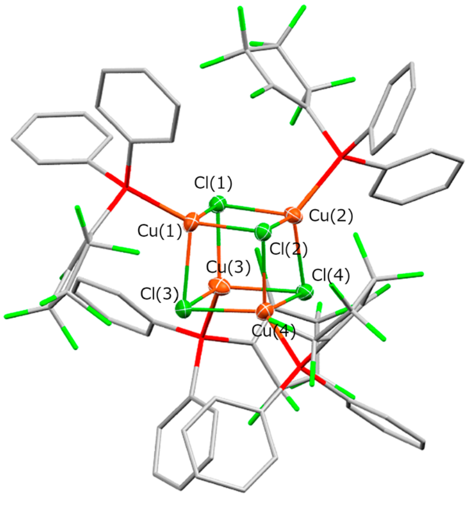

Figure 3. Molecular structure of **2a**. Thermal ellipsoids are drawn at the 50% probability level. Hydrogen atoms and disordered atoms are omitted for clarity.

Cu(I) Complexes. Reaction of copper(I) halides CuX (X = Cl, Br, I) with bisphosphine F_6PP gave the halogen-bridged dinuclear complexes $[CuX(F_6PP)]_2$ (**1a**, X = Cl; **1b**, X = Br; **1c**, X = I) (Scheme 1). Similar reactions of monophosphine F_6P with CuX yielded the tetranuclear complexes $[CuX(F_6P)]_4$ (**2a**, X = Cl; **2b**, X = Br; **2c**, X = I). The halogen-bridged dimeric form of **1c** could be cleaved by treatment with PPh_3, affording the monomeric copper(I) complex $[CuI(F_6PP)$-

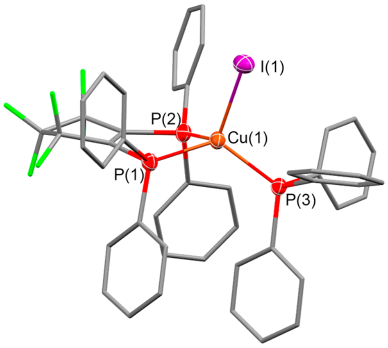

Figure 4. Structure of $3{\cdot}3CH_2Cl_2$. Thermal ellipsoids are drawn at the 50% probability level. Hydrogen atoms and the solvent molecules are omitted for clarity.

$(PPh_3)]$ (**3**). The ^{19}F NMR spectrum of **3** exhibited an ABXY spin system, showing the existence of diastereotopic ring CF_2 fluorine atoms.

The molecular structure of **1a** is shown in Figure 1, and those of **1b**,**c** are shown in Figure S1 in the Supporting Information. Selected structural parameters of **1a**−**c** are summarized in Table S1 in the Supporting Information. Complexes **1a**−**c** exhibit butterfly-like puckered $Cu_2(\mu\text{-}X)_2$ cores with distorted-tetrahedral Cu(I) ions, a well-known structural motif for copper(I) halide complexes of chelating ligands.[28] The structural parameters of **1a**−**c** are comparable to those reported for the related bisphosphine complexes $[CuX(dppBz)]_2$[29] and $[CuI(dppEt)]_2$ (Figure 2),[30] suggesting that the coordination environments around the Cu(I) centers in these complexes are similar.

The molecular structure of tetranuclear complex **2a** is shown in Figure 3, and those of **2b**,**c** are shown in Figure S2 in the Supporting Information. Complexes **2a**−**c** feature cubane-like structures containing distorted-tetrahedral Cu(I) centers, which have been observed often for Cu(I) complexes of monodentate phosphine ligands (e.g., PPh_3).[31−33] The means of the selected structural parameters for **2a**−**c** as well as of the PPh_3 analogue $[CuX(PPh_3)]_4$ (X = Cl, Br, I) are shown in Table S2 in the Supporting Information. The Cu−X and Cu−P bond lengths of **2a**−**c** are almost the same as those of the PPh_3 analogues, while a slight decrease in the mean Cu- - -Cu interatomic distances is observed for **2a**,**b**.

Table 1. Selected Structural Parameters for the Ag(I) Complexes

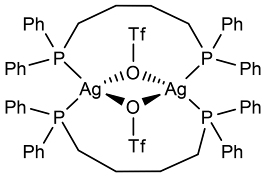

$[Ag(OTf)(dppb)]_2$

	Ag−P (Å)[a]	P−Ag−P (deg)[a,b]	θ (deg)[c]	Ag−X (Å)
4a	2.7(2)	76.5(2)	39	2.79(1)
4b	2.54(4)	82.8(7)	76	4.89(1)[d]
$[Ag(NO_3)(dppBz)_2]$[e]	2.48(3)	80.1(1)	85	8.0[d]
$[Ag(dppBz)_2](PF_6)$[f]	2.49(4)	79.6(4)	83	7.7[d]
4a(calcd)[g]	2.6(2)	78.8	44	2.698
5	2.51(4)	83.3(5)		2.4(1)
$[Ag(OTf)(dppb)]_2$[h]	2.425(3)	141.13(3)		2.73(9)

[a] Averaged values with standard deviations. [b] Intra-annular bond angle. [c] Dihedral angle between the two AgP_2 triangles. [d] Shortest interatomic distance between the Ag atom and the counterion. [e] Reference 34. [f] Reference 35. [g] Optimized structure at the B3PW91-D3/6-31G(d)-[Ag: SDD] level. [h] Reference 38.

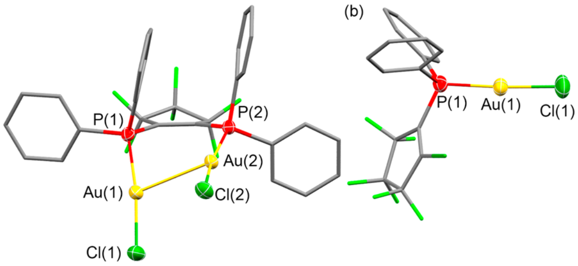

Figure 6. Molecular structures of (a) $6{\cdot}CH_2Cl_2$ and (b) **7**. Thermal ellipsoids are drawn at the 50% probability level. Hydrogen atoms and the solvent molecule are omitted for clarity.

Mononuclear Cu(I) complex **3** exhibits a highly distorted tetrahedral coordination environment around the Cu(I) ion (Figure 4). As shown in Table S1, its structural parameters are comparable to those of the dppBz analogue $[CuI(dppBz)]_2$.[29]

Ag(I) Complexes. Treatment of the bisphosphine F_6PP with $AgNO_3$ gave the bischelate complex $[Ag(F_6PP)_2](NO_3)$ (**4a**) (Scheme 1). Anion exchange of **4a** afforded the related bischelate complex $[Ag(F_6PP)_2](PF_6)$ (**4b**). In contrast, reaction of F_6PP with AgOTf afforded not the bischelate

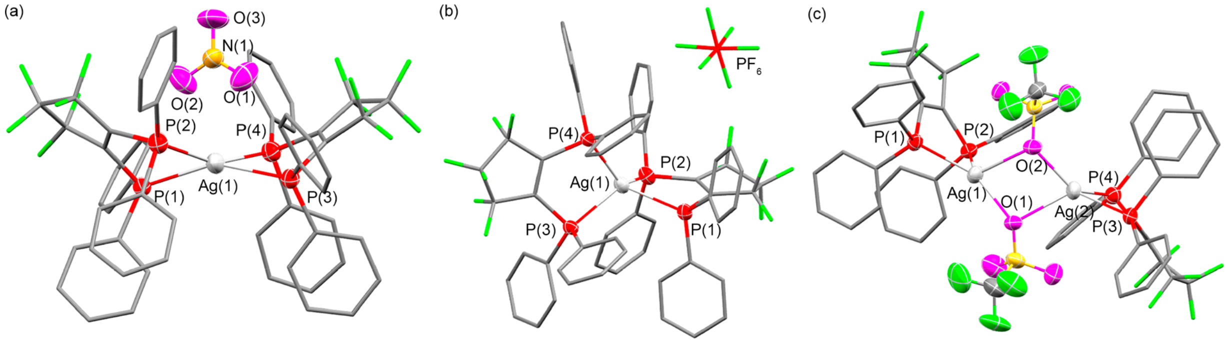

Figure 5. Structures of the Ag(I) complexes of F_6PP. Thermal ellipsoids are drawn at the 50% probability level. Hydrogen atoms are omitted for clarity. (a) **4a**. (b) $4b{\cdot}1.5CHCl_3$. One of the two independent molecules is shown. Solvent molecules and disordered fluorine atoms in the PF_6 anion are not shown. (c) $5{\cdot}CH_2Cl_2$. The solvent molecule is not shown.

DOI: 10.1021/acs.inorgchem.8b01111
Inorg. Chem. XXXX, XXX, XXX−XXX

Table 2. Selected Structural Parameters for the Au(I) Complexes

	Au−Cl (Å)[a]	P−Au (Å)[a]	P−Au−Cl (deg)[a]	Au- - -Au (Å)
6	2.287(5)	2.232(6)	170(4)	3.014(5)
7	2.277(2)	2.217(2)	176.7(1)	
$[Au_2Cl_2(dppBz)]$[b]	2.292(1)	2.239(4)	173.1(1)	2.2960(3)
$[Au_2Cl_2(dppMa)]$[c]	2.290(3)	2.231(1)	171(3)	2.97(2)
$[AuCl(PPh_3)]$[d]	2.2903(4)	2.2314(4)	179.24(1)	
6 (calcd)[e]	2.306	2.269	171.9	3.111

[a] Averaged values with standard deviations, except for those for **7** and $[AuCl(PPh_3)]$. [b] Reference 39. [c] Reference 40. [d] Reference 41. [e] Optimized structure at the B3PW91-D3/6-31G(d)[Au: SDD] level.

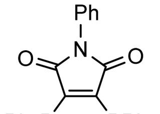
dppMa

Table 3. UV/Vis Spectral Data and TD-DFT Computational Results for the F_6PP and F_6P Complexes[a]

	λ_{max} (nm)	ε (M^{-1} cm^{-1})	λ_{calcd} (nm)[b,c]	f[b,c]	character[b,c]
1a	468	1.8×10^3	506	0.0281	Cl(3p)+Cu(3d) -π^*(C=C)
1b	462	1.9×10^3	504	0.0230	Br(4p)+Cu(3d) -π^*(C=C)
1c	454	1.3×10^3	514	0.0175	I(5p)+Cu(3d) -π^*(C=C)
2a	344	6.5×10^3	426	0.0293	Cl(3p)+Cu(3d) -π^*(C=C)
			425	0.0304	
2b	350	6.4×10^3	434	0.0254	Br(4p)+Cu(3d) -π^*(C=C)
			434	0.0254	
2c	364	9.6×10^3	448	0.0217	I(5p)+Cu(3d) -π^*(C=C)
			448	0.0217	
3	426	6.6×10^2	553	0.0006	I(5p)+Cu(3d) -π^*(C=C)
4a	378	2.0×10^3	478[d]	0.0408[d]	σ(Ag−P)- π^*(C=C)[d]
4b	376	2.1×10^3	399[e]	0.0471[e]	Ag(4d)-π^*(C=C)[e]
5	376	2.5×10^2	432	0.0278	σ(Ag−P)-π^*(C=C)[e]
			410	0.0231	
6	368	7.4×10^2	452	0.0112	Cl(3p)+Au(5d) -π^*(C=C)
7	[f]	[f]	345	0.0009	Cl(3p)+Au(5d)-π^*(C=C)

[a] Measured in CH_2Cl_2 (1 mM). [b] Calculated at the B3PW91/6-31+G(d)[Au,Ag,Cu,I: SDD] level of theory on the optimized structures. [c] S_1 state. [d] Calculated for the hexacoordinated contact ion pair $[Ag(F_6PP)_2(NO_3)]$. [e] Calculated for the free cation $[Ag(F_6PP)_2]^+$. [f] Notable absorption peaks were not observed.

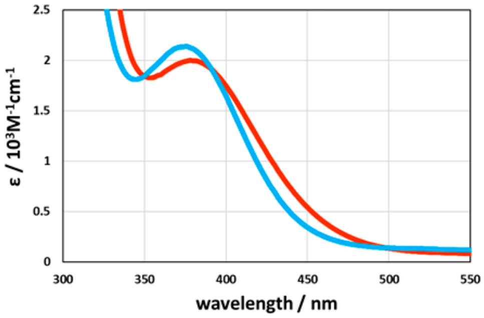

Figure 7. UV/vis absorption spectra of complexes **4a**,**b** in CH_2Cl_2: (red line) **4a**; (blue line) **4b**.

complex, but the TfO-bridged dinuclear complex $[Ag(OTf)(F_6PP)]_2$ (**5**).

Bischelate complex **4b** exhibits substantially distorted tetrahedral Ag(I) centers coordinated by two F_6PP ligands (Figure 5b). The structure of another independent molecule of **4b** is shown in Figure S3 in the Supporting Information. The Ag−P bond lengths are somewhat longer than those in the analogous dppBz complexes $[Ag(dppBz)_2](X)$ (X = NO_3,[34] PF_6[35]) (Table 1), suggesting a weaker coordinating ability for F_6PP in comparison to that of dppBz. The P−Ag−P bond angles and the dihedral angles between the two PAgP triangles (θ in Table 1) of **4b** are comparable to those found in the dppBz complexes.

In the crystal structure of **4a**, short interatomic distances between the Ag(I) center and the NO_3 anion were observed (Figure 5b), suggesting bidentate coordination of the NO_3 anion. The remarkably longer Ag−P bond lengths and the smaller θ value of **4a** in comparison to those in **4b** suggest a hexacoordinated environment for **4a**, which was corroborated by the DFT-optimized structure of **4a**.[36] Hexacoordinated Ag(I) complexes containing both P ligands and Ag−O_2NO bonds are scarce.[37] The unusual coordination mode of **4a** indicates that the π-accepting F_6PP increases the Lewis acidity of the Ag(I) center and facilitates coordination of the NO_3 anion.

AgOTf complex **5** exhibits q TfO-bridged dimeric structure (Figure 5b), resembling those observed for Cu(I) complexes **1a**−**c**. The structure of **5** can be characterized by the substantially shortened Ag−O bond lengths in comparison to those of $[Ag(OTf)(dppb)]_2$[38] (Table 1), suggesting increased

Table 4. Catalytic Hydration Reactions Using 6 or 7[a]

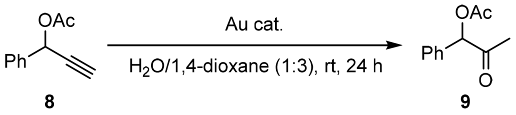

entry	Au cat. (amt (mol %))	**9** (%)	recovery of **8** (%)
1	**6** (3)	51	47
2	**6** (5)	70	30
3	**7** (3)	17	77
4	**7** (6)	35	61
5	$[Au_2Cl_2(dppBz)]$ (5)	<1	98
6[b]	**10** (3)	59	

[a] **8** (1.0 mmol). [b] Reference 20a.

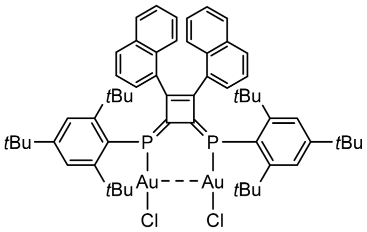

10

Lewis acidity of the Ag centers due to the electron-withdrawing F_6PP.

Au(I) Complexes. Bisphosphine F_6PP reacted with [AuCl(tht)] to yield the dinuclear Au(I) complex $[Au_2Cl_2(F_6PP)]$ (**6**) (Scheme 1). Reaction of monophosphine F_6P and AuCl(tht) afforded the mononuclear Au(I) complex $[AuCl(F_6P)]$ (**7**).

The molecular structure of **6** displays an intramolecular Au—Au short contact (Figure 6a and Table 2), indicating the existence of a weak aurophilic interaction.[1] The structural parameters of **6** are similar to those found in the related complexes $[Au_2Cl_2(dppBz)]$[39] and $[Au_2Cl_2(dppMa)]$,[40] as well as the DFT-optimized structure. The structure of complex **6** is similar to that of the PPh_3 analogue.[41]

Optical Properties of the Complexes. *Cu Complexes.* The UV/vis spectral data of the Cu(I) complexes are summarized in Table 3. UV—vis spectra of the complexes and the phosphine ligands are included in the Supporting Information. The dinuclear Cu(I) complexes **1a—c** exhibit the longest absorption maxima (λ_{max}) around 460 nm, which are attributable to (M+X)LCT excitations (X = Cl, Br, I; L = F_6PP), as judged from TD-DFT calculations. These absorptions are substantially red shifted in comparison to that of $[CuI(dppBz)]_2$ (330 nm),[29] probably because of the higher electron acceptability of F_6PP in comparison to that of dppBz. We did not observe any notable photoluminescence for these Cu(I) complexes at room temperature or at 77 K, both in solution and in the solid state, though the reason is still unclear.

Ag Complexes. As shown in Figure 7, Ag(I) complexes **4a,b** exhibit very similar UV/vis absorption spectra in CH_2Cl_2, indicating that the contact ion pair structure observed for **4a** in the solid state is not retained in solution. The λ_{max} values of **4a,b** are substantially red shifted in comparison to that of $[Ag(dppBz)_2](PF_6)$ (271 nm),[35] corroborating the π-accepting ability of F_6PP. In contrast, the dimeric structure of **5** observed in the solid state is likely retained in solution, because its longest absorption wavelength is close to that estimated by TD-DFT calculations on the optimized structure, which is similar to the crystal structure.

Au Complexes. Dinuclear Au(I) complex **6** exhibits a shoulderlike absorption at 368 nm. TD-DFT calculations suggest that the observed absorption corresponds to (M+Cl)LCT excitations. On the other hand, mononuclear complex **7** did not show any noticeable UV/vis absorption bands, probably because its longest absorption is fundamentally forbidden according to TD-DFT calculations (f = 0.0009).

Catalytic Use of the Au(I) Complexes. In order to demonstrate the potential of the F_6PP and F_6P ligands in catalysis, we investigated hydration reactions of terminal alkynes with Au(I) complexes **6** and **7** (Table 4). Gratifyingly, dinuclear complex **6** catalyzed the hydration of propargylic acetate **8** (entry 1). An increase in the catalyst loading improved the yield of **9** (entry 2). The catalytic activity of **6** is comparable to that of the diphosphinidenecyclobutene complex **10** reported by Ito et al. (entry 6).[20a] In general, molecular Au(I) complexes need preactivation using Ag(I) cocatalysts to generate the catalytically active cationic Au(I) species, and hence, complex **6** can be regarded as a rare example of an Au(I) complex functioning as a catalyst without preactivation.[42] However, mononuclear complex **7** showed only very low activity (entry 3). The yield of **9** increased proportionally to the loading of **7** (entry 4), probably excluding the intermolecular Au- - -Au interactions for **7**. A comparison of the catalytic performance of **6**, **7**, and **10** suggests the potential importance of intramolecular Au- - -Au interactions in the development of preactivation-free Au(I) catalysis.[43] In addition, the dppBz complex $[Au_2Cl_2(dppBz)]$ was effectively inactive (entry 5), indicating the importance of π-accepting ligands for high catalytic performance.

■ CONCLUSIONS

In conclusion, we have synthesized d^{10} coinage-metal complexes of the polyfluorinated bisphosphine F_6PP and monophosphine F_6P. CuX (X = Cl, Br, I) complexes of F_6PP and F_6P exhibit halogen-bridged dimeric and tetrameric structures, respectively, which are well-known for CuX complexes of bis- or monophosphines. The crystal structures of the AgX (X = NO_3, PF_6, OTf) complexes of F_6PP vary according to the nature of the counterion. The PF_6 and OTf complexes exhibit a solvent-separated ion pair structure and a TfO-bridged dimeric structure, respectively. In contrast, the $AgNO_3$ complex forms an unusual hexacoordinated structure containing a weakly coordinated NO_3 anion, indicating that the electron-withdrawing F_6PP ligand improves the Lewis acidity of the Ag(I) center. The dinuclear Au(I) complex of F_6PP shows a weak intramolecular aurophilic interaction. Without preactivation using Ag(I) cocatalysts, the Au^I-F_6PP complex catalyzes hydration of a terminal alkyne, suggesting a possible application of the polyfluorinated electron-deficient phosphines for catalysis.

■ ASSOCIATED CONTENT

Ⓢ Supporting Information

The Supporting Information is available free of charge on the ACS Publications website at DOI: 10.1021/acs.inorgchem.8b01111.

X-ray data, NMR spectra of the phosphines and the complexes, and Cartesian coordinates of the DFT-optimized structures (PDF)

Accession Codes

CCDC 1823373−1823384 contain the supplementary crystallographic data for this paper. These data can be obtained free of charge via www.ccdc.cam.ac.uk/data_request/cif, or by emailing data_request@ccdc.cam.ac.uk, or by contacting The Cambridge Crystallographic Data Centre, 12 Union Road, Cambridge CB2 1EZ, UK; fax: +44 1223 336033.

■ AUTHOR INFORMATION

Corresponding Authors

*E-mail for T.A.: tomohiro.agou.mountain@vc.ibaraki.ac.jp.
*E-mail for H.F.: hiroki.fukumoto.chem@vc.ibaraki.ac.jp.
*E-mail for T.K.: toshio.kubota.organicchem@vc.ibaraki.ac.jp.

ORCID

Tomohiro Agou: 0000-0002-9133-190X
Yoshiyuki Mizuhata: 0000-0001-5301-0024
Hiroki Fukumoto: 0000-0002-7066-3411

Notes

The authors declare no competing financial interest.

■ ACKNOWLEDGMENTS

This work was supported by JSPS KAKENHI (Grant Nos. JP15H05477, JP15K05513, and JP16K1953) and by an Ibaraki University Priority Research Grant. Computational time was provided by the Supercomputer Laboratory, Institute for Chemical Research (ICR), Kyoto University. T.A. thanks the ICR-JURC, Kyoto University, for financial support (Grant No. 2017-97). Prof. M. Minoura and Prof. K. Sugamata (Rikkyo University) are acknowledged for their kind help in the X-ray crystallographic analysis of the Ag(I) complexes.

■ REFERENCES

(1) (a) Gray, T. G.; Sadighi, J. P. Group 11 Metal-Metal Bonds. In *Molecular Metal-Metal Bonds*; Liddle, S. T., Ed.; Wiley-VCH: Weinheim, 2015; pp 397−429. (b) Sculfort, S.; Braunstein, P. Intramolecular d^{10}-d^{10} interactions in heterometallic clusters of the transition metals. *Chem. Soc. Rev.* **2011**, *40*, 2741−2760. (c) Pyykkö, P. Theoretical Chemistry of Gold. *Angew. Chem., Int. Ed.* **2004**, *43*, 4412−4456.

(2) (a) Yam, V.W.-W.; Au, V.K.-M.; Leung, S.Y.-L. Light-Emitting Self-Assembled Materials Based on d^8 and d^{10} Transition Metal Complexes. *Chem. Rev.* **2015**, *115*, 7589−7728. (b) De Angelis, F.; Fantacci, S.; Sgamellotti, A.; Cariati, E.; Ugo, R.; Ford, P. C. Electronic Transitions Involved in the Absorption Spectrum and Dual Luminescence of Tetranuclear Cubane [Cu_4I_4(pyridine)$_4$] Cluster: a Density Functional Theory/Time-Dependent Density Functional Theory Investigation. *Inorg. Chem.* **2006**, *45*, 10576−10584. (c) Cariati, E.; Bu, X.; Ford, P. C. Solvent- and Vapor-Induced Isomerization between the Luminescent Solids [CuI(4-pic)]$_4$ and [CuI(4-pic)]$_\infty$ (pic = methylpyridine). The Structural Basis for the Observed Luminescence Vapochromism. *Chem. Mater.* **2000**, *12*, 3385−3391. (d) Ford, P. C.; Vogler, A. Photochemical and Photophysical Properties of Tetranuclear and Hexanuclear Clusters of Metal with d^{10} and s^2 Electronic Configurations. *Acc. Chem. Res.* **1993**, *26*, 220−226.

(3) (a) Gorin, D. J.; Toste, F. D. Relativistic effects in homogeneous gold catalysis. *Nature* **2007**, *446*, 395−403. (b) Mao, B.; Fañanás-Mastral, M.; Feringa, B. L. Catalytic Asymmetric Synthesis of Butenolides and Butyrolactones. *Chem. Rev.* **2017**, *117*, 10502−10566. (c) Lauder, K.; Toscani, A.; Scalacci, N.; Castagnolo, D. Synthesis and Reactivity of Propargylamines in Organic Chemistry. *Chem. Rev.* **2017**, *117*, 14091−14200. (d) Pellissier, H. Enantioselective Silver-Catalyzed Transformations. *Chem. Rev.* **2016**, *116*, 14868−14917.

(4) (a) Freytag, M.; Ito, S.; Yoshifuji, M. Coordination Behavior of Sterically Protected Phosphaalkenes on the AuCl Moiety Leading to Catalytic 1,6-Enyne Cycloisomerization. *Chem. - Asian J.* **2006**, *1*, 693−700. (b) Ito, S.; Kusano, S.; Morita, N.; Mikami, K.; Yoshifuji, M. Ligand effect of buly 2,2-dialkyl-1-phosphaethenes on Au-catalyzed cycloisomerization of 1,6-enynes and lactonization of pent-4-ynoic acids. *J. Organomet. Chem.* **2010**, *695*, 291−296. (c) Ito, S.; Zhai, L.; Mikami, K. Combination of sp^2- and sp^3-Type Phosphorus Atoms for Gold Chemistry: Preparation, Structure, and Catalytic Activity of Gold Complexes That Bear Ligated 2-Silyl-1,3-diphosphapropenes. *Chem. - Asian J.* **2011**, *6*, 3077−3083.

(5) (a) Brisdon, A. K.; Herbert, C. J. Fluoroalkyl-containing phosphines. *Coord. Chem. Rev.* **2013**, *257*, 880−901. (b) Pollock, C. L.; Saunders, G. C.; Smyth, E. C. M. S.; Sorokin, V. I. Fluoroarylphosphines as ligands. *J. Fluorine Chem.* **2008**, *129*, 142−166.

(6) (a) Kim, J.; Jeong, W.; Rhee, Y. H. Flexible Tetrahydropyran Synthesis from Homopropargylic Alcohols Using Sequential Pd-Au Catalysis. *Org. Lett.* **2017**, *19*, 242−245. (b) Usui, K.; Tanoue, K.; Yamamoto, K.; Shimizu, T.; Suemune, H. Synthesis of Substituted Azulenes via Pt(II)-Catalyzed Ring-Expanding Cycloisomerization. *Org. Lett.* **2014**, *16*, 4662−4665.

(7) (a) Akahori, S.; Sakai, H.; Shinokubo, H.; Miyake, Y. Synthesis and Photodynamics of Tetragermatetrathia[8]circulene. *Org. Lett.* **2018**, *20*, 304−307. (b) Mitsudo, K.; Tanaka, S.; Isobuchi, R.; Inada, T.; Mandai, H.; Korenaga, T.; Wakamiya, A.; Murata, Y.; Suga, S. Rh-Catalyzed Dehydrogenative Cyclization Leading to Benzosilolothiophene Derivatives via Si-H/C-H Bond Cleavage. *Org. Lett.* **2017**, *19*, 2564−2564. (c) Hashimoto, T.; Kato, K.; Yano, R.; Natori, T.; Miura, H.; Takeuchi, R. Iridium-Catalyzed Synthesis of Acylpyridines by [2 + 2+2] Cycloaddition of Diynes with Acyl Cyanides. *J. Org. Chem.* **2016**, *81*, 5393−5400. (d) Korenaga, T.; Abe, K.; Ko, A.; Maenishi, R.; Sakai, T. Ligand Electronic Effect on Reductive Elimination of Biphenyl from *cis*-[Pt(Ph)$_2$(diphosphine)] Complexes Bearing Electron-Poor Diphosphines: Correlation Study between Experimental and Theoretical Results. *Organometallics* **2010**, *29*, 4025−4035. (e) Nakamura, H.; Onagi, S.; Kamakura, T. Synthesis of Heterocyclic Allenes via Palladium-Catalyzed Hydride-Transfer Reaction of Propargylic Amines. *J. Org. Chem.* **2005**, *70*, 2357−2360. (f) Cook, R. L.; Morse, J. G. 1,2-Bis[bis(pentafluorophenyl)phosphino]ethane: synthesis, characterization, and some comparisons to 1,2-bis-(diphenylphosphino)ethane. *Inorg. Chem.* **1982**, *21*, 4103−4105.

(8) (a) Korenaga, T.; Maenishi, R.; Hayashi, K.; Sakai, T. Highly Active and Enantioselective Rhodium-Catalyzed Asymmetric 1,4-Addition of Arylboronic Acid to α,β-Unsaturated Ketone by using Electron-Poor MeO-F_{12}-BIPHEP. *Adv. Synth. Catal.* **2010**, *352*, 3247−3254. (b) Korenaga, T.; Osaki, K.; Maenishi, R.; Sakai, T. Electron-Poor Chiral Diphosphine Ligands: High Performance for Rh-Catalyzed Asymmetric 1,4-Addition of Arylboronic Acids at Room Temperature. *Org. Lett.* **2009**, *11*, 2325−2328.

(9) Korenaga, T.; Ko, A.; Uotani, K.; Tanaka, Y.; Sakai, T. Synthesis and Application of 2,6-Bis(trifluoromethyl)-4-pyridyl Phosphanes: The Most Electron-Poor Aryl Phosphanes with Moderate Bulkiness. *Angew. Chem., Int. Ed.* **2011**, *50*, 10703−10707.

(10) (a) Kubota, T.; Takaki, A. Jpn. Kokai Tokko Koho JPN 2006142290, 2006;. (b) Kubota, T.; Nagasawa, T.; Hirooka, A. PCT Int. Appl. WO 2011021598 A1 20110224, 2011;. (c) Shimazaki, Y.; Ogino, M.; Kawasaki, K.; Ishii, S.; Miyauchi, A.; Kubota, T. Jpn. Kokai Tokkyo Koho, JPN 2013251315 A 20131212, 2013.

(11) Fukumoto, H.; Izumiya, H.; Kubota, T. Jpn. Kokai Tokko Koho JPN 2016060722, 2016.

(12) (a) Fukumoto, H.; Ando, M.; Shiota, T.; Izumiya, H.; Kubota, T. Efficient Synthesis of Fluorinated Phenanthrene Monomers Using Mallory Reaction and Their Polymerization. *Macromolecules* **2017**, *50*, 865−871. (b) Fukumoto, H.; Kubota, T.; Ando, M.; Shiota, T.; Izumiya, H. Jpn. Kokai Tokkyo Koho JPN 2016084448, 2016.

(13) (a) Cullen, W. R.; Harbourne, D. A.; Liengme, B. V.; Sams, J. R. Characterization of [3,3,4,4-tetrafluoro-1,2-bis(dimethylarsino)-cyclobutene] diiron hexacarbonyl and related complexes. *Inorg. Chem.* **1969**, *8*, 95−100. (b) Cullen, W. R.; Harbourne, D. A.; Liengme, B. V.; Sams, J. R. Five-coordinated iron carbonyl complexes with fluorocarbon-bridged ligands. *Inorg. Chem.* **1969**, *8*, 1464−1470. (c) Cullen, W. R.; Harbourne, D. A.; Liengme, B. V.; Sams, J. R. Novel polynuclear iron carbonyl complexes containing phosphorus and arsenic. *Inorg. Chem.* **1970**, *9*, 702−710. (d) Cullen, W. R.; Sams, J. R.; Thompson, J. A. J. Phosphine, arsine, and stibine derivatives of $(\pi\text{-}C_5H_5)Fe(CO)_2SnR_3$. Nature of the iron-tin bond. *Inorg. Chem.* **1971**, *10*, 843−850. (e) Einstein, F. W. B.; Restivo, R. A fluoroalicyclic-bridged ditertiary phosphine derivative of iron. The crystal structure of $(\pi\text{-}C_5H_5)Fe(CO)(f6fos)SnMe_3$. *Inorg. Chim. Acta* **1971**, *5*, 501−510. (f) Harrison, W.; Trotter, J. Crystal and molecular structure of [1,2-bis(diphenylphosphino)hexafluorocyclopentene]-dinitrosyliron. *J. Chem. Soc. A* **1971**, 1542−1546.

(14) Stockel, R. F. Reactions of 1,2-dichlorohexafluorocyclopentene with secondary phosphines. *Can. J. Chem.* **1968**, *46*, 2625−2628.

(15) Cullen, W. R.; Williams, M. The reaction of $R_2PC = CCl(CF2)_n$ with iron carbonyls. Unusual complexes formed by ligand cleavage reactions. *Can. J. Chem.* **1980**, *58*, 143−150.

(16) (a) Cullen, W. R.; Thompson, J. A. J. Fluorocarbon-bridged ditertiary phosphine derivatives of rhodium carbonyl halides. *Can. J. Chem.* **1970**, *48*, 1730−1735. (b) Einstein, F. W. B.; Hampton, C. R. S. M. The Crystal Structure of $[Rh(f_6fos)_2]^+[cis\text{-}(CO)_2RhCl_2]^-$. *Can. J. Chem.* **1971**, *49*, 1901−1910.

(17) Cullen, W. R.; Dong, D. F.; Thompson, J. A. J. Fluorocarbon-bridged di(tertiary phosphine) complexes of Group VIB metal carbonyls. *Can. J. Chem.* **1969**, *47*, 4671−4677.

(18) Minato, M.; Miyato, Y.; Kakeya, M. Molecular Structure of $Co_2(\mu\text{-Alkyne})$ Complex Containing $Ph_2PC_5F_6PPh_2$ Ligand. *Int. J. Org. Chem.* **2015**, *05*, 119−125.

(19) (a) Holz, J.; Schaeffner, B.; Zayas, O.; Spannenberg, A.; Boerner, A. Synthesis of Chiral 2-Hydroxy-1-methylpropanoates by Rhodium-Catalyzed Stereoselective Hydrogenation of α-(Hydroxymethyl)-acrylate Derivatives. *Adv. Synth. Catal.* **2008**, *350*, 2533−2543. (b) Holz, J.; Zayas, O.; Jiao, H.; Baumann, W.; Spannenberg, A.; Monsees, A.; Riermeier, T. H.; Almena, J.; Kadyrov, R.; Boerner, A. A Highly Tunable Family of Chiral Bisphospholanes for Rh-Catalyzed Enantioselective Hydrogenation Reactions. *Chem. - Eur. J.* **2006**, *12*, 5001−5013.

(20) (a) Ito, S.; Nanko, M.; Mikami, K. π-Extended DPCB for Activation-Free Homogeneous Gold Catalysis. *ChemCatChem* **2014**, *6*, 2292−2297. (b) Ito, S.; Shinozaki, T.; Mikami, K. Stereoselective Catalytic Synthesis of Alkynylated Phosphaethenes Leading to Activation-Free Gold Catalysis. *Eur. J. Org. Chem.* **2017**, *2017*, 6889−69900.

(21) Pangborn, A. B.; Giardello, M. A.; Grubbs, R. H.; Rosen, R. K.; Timmers, F. J. Safe and Convenient Procedure for Solvent Purification. *Organometallics* **1996**, *15*, 1518−1520.

(22) Uson, R.; Laguna, A.; Laguna, M. (Tetrahydrothiophene)-Gold(I) or Gold(III) Complexes. *Inorg. Synth.* **2007**, *26*, 85−91.

(23) Hang, X.-C.; Gu, W.-P.; Chen, Q.-Y.; Xiao, J.-C. Reaction of dfluorocarbene with propargyl esters and efficient synthesis of difluorocyclopropyl ketones. *Tetrahedron* **2009**, *65*, 6320−6324.

(24) Sheldrick, G. M. Crystal structure refinement with *SHELXL*. *Acta Crystallogr., Sect. C: Struct. Chem.* **2015**, *71*, 3−8.

(25) Frisch, M. J., et al.. *Gaussian 16, Revision A.03*; Gaussian, Inc., Wallingford, CT, 2016. See the Supporting Information for the complete citation.

(26) Grimme, S.; Antony, J.; Ehrlich, S.; Krieg, H. A consistent and accurate ab initio parametrization of density functional dispersion correction (DFT-D) for the 94 elements H-Pu. *J. Chem. Phys.* **2010**, *132*, 154104.

(27) Park, J. D.; Bertino, C. D.; Nakata, B. T. Chemistry of 1-lithio-2-chloroperfluorocycloalkenes. *J. Org. Chem.* **1969**, *34*, 1490−1492.

(28) (a) Gibbons, S. K.; Hughes, R. P.; Glueck, D. S.; Royappa, A. T.; Rheingold, A. L.; Arthur, R. B.; Nicholas, A. D.; Patterson, H. H. Synthesis, Structure, and Luminescence of Copper(I) Halide Complexes of Chiral Bis(phosphines). *Inorg. Chem.* **2017**, *56*, 12809−12820. (b) Tsuge, K.; Chishina, Y.; Hashiguchi, H.; Sasaki, Y.; Kato, M.; Ishizaka, S.; Kitamura, N. Luminescence copper(I) complexes with halogenido-bridge dimeric core. *Coord. Chem. Rev.* **2016**, *306*, 636−651. (c) Peng, R.; Li, M.; Li, D. Copper(I) halides: A versatile family in coordination chemistry and crystal engineering. *Coord. Chem. Rev.* **2010**, *254*, 1−18. (d) Ford, P. C.; Cariati, E.; Bourassa, J. Photoluminescence Properties of Multinuclear Copper(I) compounds. *Chem. Rev.* **1999**, *99*, 3625−3648.

(29) Tsuboyama, A.; Kuge, K.; Furugori, M.; Okada, S.; Hoshino, M.; Ueno, K. Photophysical Properties of Highly Luminescent Copper(I) Halide Complexes Chelated with 1,2-Bis-(diphenylphosphino)benzene. *Inorg. Chem.* **2007**, *46*, 1992−2001.

(30) Aslanidis, P.; Cox, P. J.; Divanidis, S.; Karagiannidis, P. Copper(I) halide complexes from *cis*-1,2-bis(diphenylphosphino) ethylene and some heterocyclic thiones. *Inorg. Chim. Acta* **2004**, *357*, 1063−1076.

(31) Churchill, M. R.; Kalra, K. Molecules with an M4 × 4 core. I. Crystal and molecular structure of tetrameric triphenylphosphinecopper(I) chloride, a cubane-like molecule, including the location and refinement of all hydrogen atoms. *Inorg. Chem.* **1974**, *13*, 1065−1071.

(32) Barron, P.; Dyason, J. C.; Engelhardt, L. M.; Healy, P. C.; White, A. H. Lewis base adducts of Group IB metal compounds. 8. High-resolution solid-state phosphorus-31 nuclear magnetic resonance spectra of tetrameric ((triphenylphosphine)copper(I) halide) complexes and crystal structure determination of "cubane" $[PPh_3CuBr]_4$. *Inorg. Chem.* **1984**, *23*, 3766−3769.

(33) Perruchas, S.; Tard, C.; Le Goff, X. F.; Fargues, A.; Garcia, A.; Kahlal, S.; Saillard, J.-Y.; Gacoin, T.; Boilot, J.-P. Thermochromic Luminescence of Copper Iodide Clusters: The Case of Phosphine Ligands. *Inorg. Chem.* **2011**, *50*, 10682−10692.

(34) Matsumoto, K.; Shindo, T.; Mukasa, N.; Tsukuda, T.; Tsubomura, T. Luminescent Mononuclear Ag(I)-Bis(diphosphine) Complexes: Correlation between the Photophysics and the Structures of Mononuclear Ag(I)-Bis(diphosphine) Complexes. *Inorg. Chem.* **2010**, *49*, 805−814.

(35) Osawa, M.; Hoshino, M. Photochemistry and photophysics of the tetrahedral silver (I) complex with diphosphine ligands: $[Ag(dppb)_2]PF_6$ (dppb = 1,2-bis[diphenylphosphino]benzene). *Chem. Commun.* **2008**, 6384−6386.

(36) Hexacoordinated Ag(I) complexes containing a chelating NO_3 ion: (a) Cardoso, J. M. S.; Correia, I.; Galvão, A. M.; Marques, F.; Carvalho, M. F. N. N. Synthesis of Ag(I) camphor sulphonylimine complexes and assessment of their cytotoxic properties against *cisplatin*-resistant A2780cisR and A2780 cell lines. *J. Inorg. Biochem.* **2017**, *166*, 55−63. (b) Barwiolek, M.; Babinska, M.; Kozakiewicz, A.; Wojtczak, A.; Kaczmarek-Kedziera, A.; Szlyk, E. Structural and spectral studies of silver(I) complexes with new Schiff bases derived from 2-thiopheneethylamine and their application in thin layer deposition by spin and dip coating techniques. *Polyhedron* **2017**, *124*, 12−21. (c) Tashiro, S.; Tanihira, J.-I.; Yamada, M.; Shionoya, M. Discrete and Polymeric, Mono- and Dinuclear Silver Complexes of a Macrocyclic Tetraoxime Ligand with Ag^I-Ag^I Interactions. *Sensors* **2013**, *13*, 5671−5685. (d) Barceló-Oliver, M.; Estarellas, C.; Terrón, À.; García-Raso, Á.; Frontera, A. RNA's uracil quartet model with a non-essential metal ion. *Chem. Commun.* **2011**, *47*, 4646−4648.

(37) Ag(I) complexes containing P ligands and a coordinating NO_3 anion: (a) Gao, S.; Li, Z.-F.; Liu, M.; Jin, Q.-H.; Chen, Y.; Deng, Z.-J.; Zhang, Z.-W.; Zhang, C.-L. A series of silver(I) complexes with bis[2-(diphenylphosphino)phenyl]ether (DPEphos) and bis-(diphenylphosphino)ethane (dppe): Synthesis, structural characterization and photophysical properties. *Polyhedron* **2014**, *83*, 10−15. (b) Lozano, E.; Nieuwenhyzen, M.; James, S. L. Ring-Opening Polymerisation of Silver-Diphosphine $[M_2L_3]$ Coordination Cages To Give $[M_2L_3]_\infty$ Coordination Polymers. *Chem. - Eur. J.* **2001**, *7*, 2644−2651. (c) Bachechi, F.; Burini, A.; Galassi, R.; Pietroni, B. R.; Tesei, D. A Single-Strand Helical Motif Induced by Self-Assembly of

DOI: 10.1021/acs.inorgchem.8b01111

$[Ag(TFP)]^+$ Moieties with Nitrate Anions – ^{31}P NMR Spectroscopic and X-ray Crystal Structure Characterization of the Complexes Involved in Equilibrium Reactions of Silver Salts and TFP Ligand. *Eur. J. Inorg. Chem.* **2002**, *2002*, 2086−2093. (d) Khan, Md. N. I.; Staples, R. J.; King, C.; Fackler, J. P., Jr.; Winpenny, R. E. P. Syntheses and X-ray structural characterization of three-coordinate gold(I) and silver(I) complexes with the potentially tetradentate ligand tris(2-(diphenylphosphino)ethyl)amine (NP_3): $[Au_2(NP_3)_2](BPh_4)_2$, $Au(NP_3)PF_6$, $Au(NP_3)NO_3$, $Ag(NP_3)NO_3$, and $Ag(NP_3)PF_6$. The Au(I) compounds are luminescent. *Inorg. Chem.* **1993**, *32*, 5800−5807. (e) Kuang, S.-M.; Zhang, L.-M.; Zhang, Z.-Z.; Wu, B.-M.; Mak, T. C. W. Synthesis and structural characterization of binuclear silver(I) complexes bridged by three polydentate phosphine ligands. *Inorg. Chim. Acta* **1999**, *284*, 278−283.

(38) Cui, L.-N.; Li, Z.-F.; Jin, Q.-H.; Xin, X.-L.; Zhang, C.-L. Honeycomb" (6,3) network constructed from 14-membered ring $[Ag_2(\mu\text{-dppb})_2]$: Synthesis, characterization and crystal structures of two silver(I) complexes of bis(diphenylphosphino)butane. *Inorg. Chem. Commun.* **2012**, *20*, 126−130.

(39) (a) Yoshinari, N.; Kitani, N.; Tsukuda, T.; Konno, T. [μ-1,2-Bis(diphenylphosphanyl)benzene-κ^2P:P']bis[chlorogold(I)]. *Acta Crystallogr., Sect. E: Struct. Rep. Online* **2011**, *67*, m121. (b) Mohamed, A. A.; Krause Bauer, J. A.; Bruce, A. E.; Bruce, M. R. M. [μ-*o*-Phenylenebis(diphenylphosphine)-κ^2P:P']bis[chlorogold(I)], dppbz-$(AuCl)_2$. *Acta Crystallogr.* **2003**, *C59*, m84−m86.

(40) Nyamwihura, R.; Yang, L.; Nesterov, V. N.; Richmond, M. G. Diphosphine-bridged digold(I) compounds: Structural and computational studies on the aurophilic interaction in $Au_2Cl_2(\mu\text{-bpcd})$ and $Au_2Cl_2(\mu\text{-bmi})$. *J. Mol. Struct.* **2017**, *1129*, 188−194.

(41) Borissova, A. O.; Koriyukov, A. A.; Antipin, M. Y.; Lyssenko, K. A. Estimation of Dissociative Energy in Donor-Acceptor Complex $AuCl{\cdot}PPh_3$ via Topological Analysis of the Experimental Electron Density Distribution Function. *J. Phys. Chem. A* **2008**, *112*, 11519−11522.

(42) Au cluster catalyzed alkyne hydration: (a) Oliver-Meseguer, J.; Cabrero-Antonino, J. R.; Domínguez, I.; Leyva-Pérez, A.; Corma, A. Small Gold Clusters Formed in Solution Give Reaction Turnovers of 10^7 at Room Temperature. *Science* **2012**, *338*, 1452−1455. (b) Hashmi, A. S. K. Sub-Nanosized Gold Catalysts. *Science* **2012**, *338*, 1434.

(43) Weber, D.; Gagné, M. R. Aurophilicity in Gold(I) Catalysis: For Better or Worse? *Top. Curr. Chem.* **2014**, *357*, 167−212.

DOI: 10.1021/acs.inorgchem.8b01111
Inorg. Chem. XXXX, XXX, XXX−XXX